Current Research in Food Science 5 (2022) 1616–1624

Contents lists available at ScienceDirect

Current Research in Food Science

journal homepage: www.sciencedirect.com/journal/current-research-in-food-science

Plasma-activated water promoted the aggregation of *Aristichthys nobilis* myofibrillar protein and the effects on gelation properties

Mengzhe Li [a,1], Tong Shi [a,1], Xin Wang [a], Yulong Bao [a], Zhiyu Xiong [a], Abdul Razak Monto [a], Wengang Jin [b], Li Yuan [a,**], Ruichang Gao [a,b,*]

[a] School of Food and Biological Engineering, Jiangsu University, Zhenjiang, Jiangsu Province, 212013, China
[b] Bio-resources Key Laboratory of Shaanxi Province, School of Bioscience and Engineering, Shaanxi University of Technology, Hanzhong, 723001, PR China

ARTICLE INFO

Handling Editor: Dr. Quancai Sun

Keywords:
Plasma-activated water
Myofibrillar proteins
Gelling properties
Secondary structures
Hydrophobic interaction
ζ-potential

ABSTRACT

Plasma is a new technology used to modify myofibrillar proteins (MPs) structure and promote protein aggregation. In order to study the mechanism of plasma modifying MPs thus the effects on qualities of MP gels, MPs were extracted by 0.6 M NaCl solution prepared with plasma-activated water (PAW) at different treatment time (0 s, 30 s, 60 s, 120 s, 240 s). With the prolonged PAW treatment time from 0 to 240 s, the pH values of natural MP solutions decreased significantly from 5.91 to 2.61 ($P < 0.05$), the H_2O_2 concentration in PAW increased from 0 to 70.82 μg/L ($P < 0.05$), and the net negative charges of MPs first decreased and then increased ($P < 0.05$). In addition, PAW caused significantly ($P < 0.05$) weakened ionic bonds and enhanced hydrophobic interactions, which promoted the aggregation and gelation of MPs thus forming MP gel with higher gel strength and a denser three-dimensional network. Furthermore, Raman spectra and intrinsic fluorescence suggested that PAW promoted the unfolding of MP structures and transformation from α-helixes and random coils to β-sheets and β-turns. Dynamic rheology indicated a gradually increased storage modulus and shortened degradation time of MPs with an increasing treatment time of PAW. Furthermore, PAW modification significantly improved the water holding capacity of MPs gels. These results demonstrated that the declined pH of MP solutions induced by PAW and increased H_2O_2 in PAW altered the ζ-potential of MP solutions and promoted the unfolding and aggregation of MPs during heating *via* hydrophobic interactions, ultimately enhancing gelling properties of MPs. The present work suggested the potential use of PAW in preparing freshwater MP gels with high quality.

1. Introduction

Surimi-based products are potentially significant sources of healthy food products in the human diet due to their high protein and low-fat characteristics (Fang et al., 2021). The quality of surimi-based products depends on the unfolding of myofibrillar proteins (MPs) and the subsequent heat-induced aggregation driven by intermolecular forces (Cao et al., 2018). According to 'The State of World Fisheries and Aquaculture (2022)' of the statistics by FAO, the aquaculture quantity of silver carp increased to 4896.6 thousand tons by 2020 (*The State of World Fisheries and Aquaculture 2022*, 2022). The output of surimi products in China has grown rapidly in recent years and is about 1,334, 200 tons in 2021, of which the annual export quantity is 134,100 tons (https://www.chyxx.com/industry/1117921. html). Furthermore, China is the largest freshwater fish farming country of the world. Bighead carp (*Aristichthys nobilis*) is one of the famous freshwater fishes in China and a tremendous potential raw material for surimi. However, *Aristichthys nobilis* was once thought to be a 'very difficult to gel' species (Xiong et al., 2021). Nowadays, surimi products with nutrient retention and enhanced gels are needed as consumer mouthfeel requirements for surimi and surimi-based products have changed and increased. Therefore, researchers are creating ways to enhance the gelling properties of freshwater fish to produce surimi products with desirable quality attributes (Ma et al., 2018; Qian et al., 2021).

Various food-grade additives and cross-linking enzymes have been used. Phenolic compounds such as tannic acid, catechin and ferulic acid have been reported to be used as protein cross-linking agents to improve the breaking force and deformation of surimi from bigeye snapper and

* Corresponding author. School of Food and Biological Engineering, Jiangsu University, No. 301, Xuefu Road, Zhenjiang, Jiangsu Province, 212013, China.
** Corresponding author.
E-mail addresses: yuanli24@163.com (L. Yuan), xiyuan2008@ujs.edu.cn (R. Gao).
[1] These authors contributed to the work equally and should be regarded as co-first authors.

https://doi.org/10.1016/j.crfs.2022.09.003
Received 4 August 2022; Received in revised form 30 August 2022; Accepted 2 September 2022
Available online 15 September 2022

mackerel (Maqsood et al., 2013). However, the oxidation of phenolic compounds from *ortho*-diphenol into an *ortho*-quinone form may adversely affect the quality of surimi by reducing aroma components and antioxidant activity (Nikolantonaki et al., 2014). Furthermore, various food-grade ingredients can be added to improve the gel properties of surimi, such as konjac glucomannan (Xiong et al., 2009), and starch (Kong et al., 2016) used as fillers and extenders. Nevertheless, these ingredients may adversely cause surimi products to develop discoloration or odors (Fang et al., 2021). In addition, there are also many kinds of researches focusing on processing methods, such as the use of microwave heating (Wang et al., 2019); high-pressure hydrostatic technology (HHP) (Qiu et al., 2013); microwave-water bath combination (Jiao et al., 2019). However, microwave heating makes the gel surface dry and rough, and a better gel morphology could not be obtained (Cao et al., 2018). The processing of surimi products through HHP and other methods has extremely high requirements on equipment. Due to the unique texture properties and high nutritional value of surimi, the demand for high-quality surimi products is increasing. Therefore, it is necessary to explore new methods for producing freshwater surimi products with high-quality.

Plasma is known as the fourth state of matter, Plasma-activated water (PAW) can be obtained by applying high pressure to air through a plasma jet and then ionizing distilled water, which contains a large number of active substances including NO_3^-, NO_2^-, H_2O_2 and reactive oxygen and nitrogen species (RONS) (Qian et al., 2021). PAW has garnered increasing interest in recent years due to its low cost, easy preparation and no residue (Qian et al., 2021). PAW can affect the structure and properties of starch and is expected to increase resistant starch content (Laurita et al., 2021). PAW can also be used in the sterilization and preservation of foods such as shrimps (*Metapenaeus ensis*) (Liao et al., 2018), rocket leaves (Laurita et al., 2021), Asian sea bass (*Lates calcarifer*) (Chaijan et al., 2021), etc., to retain food nutrients and extend shelf life. In addition, Qian et al. (2021) has also shown that PAW can prepare chicken myofibrillar protein gels (CMPs) with intrinsic antibacterial activity. However, to date, few studies have been published on the effects of PAW on the quality of freshwater surimi products.

In the present work, MPs extracted from *Aristichthys nobilis* were solubilized in a salt solution prepared by PAW instead of the traditional deionized water. This work aimed to evaluate the effects of PAW with various treatment time on the heat-induced aggregation and gelling properties of MP and provide a low-cost new solution for improving the quality of freshwater surimi products.

2. Materials and methods

2.1. Materials

Fresh *Aristichthys nobilis* weighing (1.5 ± 0.2) kg was purchased from Jimailong supermarket in Zhenjiang, Jiangsu Province, China. After being quickly killed by professionals in the supermarket, the *Aristichthys nobilis* was put into ice and brought back to the laboratory within 20 min. All of the analytical grade chemicals were purchased from Sinopharm Chemical Reagent Co., Ltd. (Shanghai, China).

2.2. Preparation of PAW

PAW was prepared according to Qian et al. (2021) using a high performance digitized plasma generator (PG-1000 ZD, Suman Plasma Technology Co., Ltd., Nanjing, China). The plasma spray gun was placed about 10 cm below 300 mL of deionized water and exposed to the plasma jet for 0 s, 30 s, 60 s, 120 s and 240 s to obtain PAW, which was stored at 4 °C for no more than 48 h for subsequent preparation of myofibrillar protein.

2.3. Extraction of myofibrillar proteins

The MP was extracted according to a previous method with minor modifications (Gao et al., 2019). The white meat of fresh *Aristichthys nobilis* was evenly ground with a meat grinder and divided into five equal parts, then cold 0.1 M Sodium chloride (NaCl)-Tris-HCl buffer (pH = 7.0) was added (m: v = 1: 5). The fish meat soaked in buffer was homogenized at 10,000 r/min for 2 min at 4 °C using a T25 Ultra-turrax homogenizer (IKA Labortechnik, Staufen, Germany). After homogenization, the solution was centrifuged at 10,000 g for 15 min at 4 °C using a CR21N high-speed centrifuge (Eppendorf Himac Technologies Co., Japan), and the supernatant was discarded. 0.1 M NaCl Tris-HCl buffer solution was added to the precipitate and the above steps were repeated twice. Sodium chloride powder was dissolved in the above-prepared PAW solutions (0 s, 30 s, 60 s, 120 s, 240 s) to prepare 0.6 M NaCl-PAW solutions, which were added to the obtained MP precipitates (m: v = 1: 3) and homogenized. Then the suspensions were centrifuged and the collected supernatants were solubilized MPs named PAW_0, PAW_{30}, PAW_{60}, PAW_{120}, and PAW_{240}, respectively. The Biuret method was used to determine the protein concentration of MP solutions (Zhang et al., 2022).

2.4. Preparation of MP gels

The preparation of MP gels refers to the method of Shi et al. (2020) with slight modifications. The extracted MP solutions were adjusted to the protein concentration of 30 mg/mL with the prepared PAW (0 s, 30 s, 60 s, 120 s, and 240 s). 20 mL MP solution was poured into a flat bottom centrifuge tube and placed in a 40 °C water bath for 60 min with a subsequent water bath at 90 °C for 30 min. Then, the heated samples were rapidly cooled in ice water and placed in a 4 °C refrigerator for 12 h to obtain MP gels named PAW_0, PAW_{30}, PAW_{60}, PAW_{120} and PAW_{240}, respectively.

2.5. pH and zeta potential (ζ-potential)

The pH values of MP solutions were measured using a pH meter (PHSJ-3F, Shanghai INESA Scientific Instrument Co., Ltd., China). ζ-potential was measured using a dynamic light scattering-Zeta potential instrument (NanoBrook 90 Plus PALS, USA). The protein concentration in the measurement of both pH and ζ-potential was 0.1 mg/mL. Specially, to avoid the pH effects induced by PAW, the MP solutions used to the measurement of ζ-potential was adjusted by 0.6 M NaCl solution prepared by deionized water. The changes in ζ-potential of MPs at Stage 1 (25 °C 30 min), Stage 2 (40 °C 60 min) and Stage 3 (40 °C 60 min + 90 °C 30 min) were measured, and three parallels were set for each sample.

2.6. H_2O_2 concentration in PAW

H_2O_2 concentration in PAW was measured according to the method described by Klassen et al. (1994) with slight modifications. 3.4 g $KMnO_4$ was accurately weighted then solubilized in 500 mL distilled water, which was kept slightly boiling for 1 h. After being cooled, the solution was filtered through a microporous glass funnel, then the filtrate was diluted to 1L and placed in a brown reagent bottle. 0.2 g sodium oxalate was accurately weighted into a 250 mL conical flask, 80 mL distilled water and 20 mL sulfuric acid solution (sulfuric acid: water = 1:4) were added. Subsequently, this solution was heated to 80 °C and titrated with $KMnO_4$. The temperature of the liquid was kept at 60–70 °C near the end point, and the titration would not end until the pink color did not disappear for 30 s. The concentration of $KMnO_4$ standard solution was calculated as the following formula (1):

$$C\left(\frac{1}{5}KMnO_4\right) = \frac{M(Na_2C_2O_4)}{V(KMnO_4)} \times 0.067 \quad (1)$$

In the formula (1), M($Na_2C_2O_4$) was sodium oxalate 0.2 g, V($KMnO_4$) was the volume of potassium permanganate used, C(1/5$KMnO_4$) was the concentration of potassium permanganate standard solution.

25 mL PAW (0 s, 30 s, 60 s, 120 s, 240 s) was titrated with $KMnO_4$ standard titration, and maintained for 30 s without fading. The concentration of H_2O_2 was calculated by the following formula (2):

$$\rho(H_2O_2)\left(\frac{\mu g}{L}\right) = \frac{C_{(KMnO_4)} - \left[V_{(KMnO_4)} - V_0\right] \times 10^{-3} \times M_{\left(\frac{1}{2}H_2O_2\right)}}{V_{PAW}} \quad (2)$$

In the formula (2), V($KMnO_4$) was the volume of potassium permanganate used to titrate PAW, V_0 was the volume of $KMnO_4$ used in the blank group, V_{PAW} was the volume of plasma activated water 25 mL, M (1/2H_2O_2) was half of the molar mass of hydrogen peroxide 17 g/mol.

2.7. Molecular forces

The measurement of molecular forces was according to Xiong et al. (2021) with minor changes. Four copies of 2.0 g MP gel samples were homogenized respectively at 10,000 r/min for 2 min in 10 mL of the following reagents: 0.05 mol/L NaCl (S1); 0.6 mol/L NaCl (S2); 0.6 mol/L NaCl, 1.5 mol/L Urea (S3); 0.6 mol/L NaCl, 8 mol/L Urea (S4). The homogenate was stirred for 1 h at 4 °C and then centrifuged at 10, 000 g for 15 min. Protein concentrations were determined by the Coomassie brilliant blue method (Karimi et al., 2022). The difference in protein concentration between S2 and S1 solutions represented the contribution of ionic bonds; the difference in protein concentration between S3 and S2 solutions represented the contribution of hydrogen bonds; the difference in protein concentration between S4 and S3 solutions represented the contribution of hydrophobic interactions. Results were expressed in mg soluble protein/mL of homogenate.

2.8. Raman spectroscopy

A previous method by Xu et al. (2011) was referred with some modifications for the detection of Raman spectroscopy. Each PAW-treated sample under different heating treatments was pre-cooled in a −40 °C refrigerator for more than 4 h and then freeze-dried for 48 h using vacuum freeze-drying equipment (Boyikang Co., Ltd., Beijing, China). Laser Raman microscopy (DXR, Thermo Co., Waltham, MA, USA) was used at an excitation wavelength of 532 nm. The spectral resolution was 2 cm^{-1}. Samples were placed on glass slides focused around 10 mW. Spectra were recorded in the 600-3200 cm^{-1} range. Spectrogram processing was performed on OMNIC 8.0 software. In detail, multi-point baseline correction was performed to remove the fluorescence background, and then smoothing was performed, and the 1600-1700 cm^{-1} band was selected for storage. Deconvolution and second-order derivation were performed using Peak Fit 4.12 software to distinguish overlapping sub-peaks, continuous fitting minimized errors, peak intensities and areas were obtained, and amide I was characterized by calculation with secondary structure changes.

2.9. Intrinsic fluorescence intensity (IFI)

Intrinsic fluorescence was measured as describe by Shi et al. (2019) with minor modification. The MPs solution was diluted to 0.01 mg/mL firstly and then scanned in a fluorescence spectrophotometer (F-7100 FL Spectrophotometer, Hitachi, Japan). IFI was obtained between 300 and 400 nm at an excitation wavelength of 295 nm with a scanning speed of 1000 nm/min. The excitation and emission slit widths were 10 nm.

2.10. Protein aggregation

The protein aggregation measurement was according to a previous study (Gao et al., 2019) with slight modifications. The MP solutions were adjusted to a protein concentration of 1.0 mg/mL with the prepared PAW (0 s, 30 s, 60 s, 120 s, 240 s). The MP solutions were stabilized to room temperature after Stage 1, Stage 2, Stage 3 heating treatment. The absorbance at 340 nm of the treated protein solution was measured using a UV–Vis7600 spectrophotometer (Shanghai Prism Technology Co., China). Three parallels were set for each sample.

2.11. Gel strength

A TAXT Plus texture analyzer (Stable Micro Systems Co., Surrey, UK) equipped with a P/5 probe was used (Fang et al., 2021). The test conditions were as follows: the pre-test speed was 2.00 mm/s; the test speed was 2.00 mm/s; the post-test speed was 4.00 mm/s; the distance was 50 mm; the trigger force was 2.0 g. The breaking force (g) and deformation (mm) of MP gels was measured under 25 °C. Five parallels were set for each sample, and the gel strength was calculated as the following:

2.12. Water holding capacity

The WHC of MP gel samples was measured according to the method of Li et al. (2019). 3.0 g gel was placed in a centrifuge tube (m_0) and weighed together as m_1. The weighed samples were immediately placed in a centrifuge (Eppendorf 5810, Hamburg, Germany) at 10,000 g for 5 min at 4 °C. The tube with the pellet was inverted for 10 min after the supernatant was discarded, which can make the supernatant better drained. Subsequently, the remaining water on the surface was blotted with filter paper, then the centrifuge tube containing the gel was accurately weighed as m_2. The following equation was used to calculate the WHC:

2.13. Dynamic rheological analysis

The rheological properties of MPs were measured using a rheometer (Discovery HR-1, TA Instruments Co., Ltd., New Castle DE, USA)with a 40 mm flat plate model. The samples were heated from 20 °C to 90 °C at a heating rate of 2 °C/min and then cooled from 90 °C to 20 °C at 4 °C/min. A gap of 1 mm was set between the sample and the fixture, and silicone oil was applied to the outer edge to prevent water evaporation. The rheological behavior of the samples was measured using a dynamic vibration frequency of 1000 Hz, and the storage modulus of the samples was expressed as G'. Three parallels were set for each sample.

2.14. Laser confocal microscopy (CLSM) analysis

According to the method described by Song et al. (2022) with slight modifications, a Leica TCS SP8 confocal microscope (Leica Microsystems Inc., Heidelberg, Germany) was used for laser confocal analysis. 1 mL MP gel or its sol was mixed with 10 mg/mL fast green and stained for 1 h. 60 μL of the mixed sample was placed on a glass slide, covered with a coverslip, and placed upside down on a loading table for observation. The excitation wavelength was set at 633 nm to detect Fast Green (stained protein).

2.15. Statistical analysis

SPSS 17.0 software (SPSS 17.0 for windows, SPSS Inc, Chicago, IL, USA) was used for significant difference analysis ($P < 0.05$). One-way ANOVA and Tukey's test were used to assess statistical differences and graphs were drawn using Origin 9.0 (Origin Lab Co., Northampton, MA, USA).

3. Results

3.1. pH, ζ-potential and H_2O_2 content

To study the changes in net charges and pH values of MP solutions after PAW treatment, pH and ζ-potential analysis were performed. With

the treatment time increased from 0 to 240 s, the pH significantly ($P < 0.05$) decreased from 5.91 to 2.61 at Stage 1, 5.59 to 2.58 at Stage 2, 5.56 to 2.54 at Stage 3, respectively (Fig. 1(a)). These results demonstrated that PAW significantly reduced the pH values of MP solution owing to its acidic property (S. Fig. 1), which was consistent with the previous reports (Qian et al., 2019). Simultaneously, the ζ-potential was changed from initial −5.4 mV of PAW_0 to −2.4 mV of PAW_{120} at Stage 1, -4.7 mV of PAW_0 to −1.8 mV of PAW_{120} at Stage 2, -4.0 mV of PAW_0 to −1.7 mV of PAW_{60} at Stage 3 ($P < 0.05$), respectively (Fig. 1 (b)).

The plasma jet ionizes air to generate a part of H_2O_2 (Qian et al., 2021), which can oxidatively modify MPs. The present study explored the modification degree by detecting the change of H_2O_2 concentration in PAW with the prolongation of treatment. The concentration of H_2O_2 increased significantly ($P < 0.05$) from 8.73 μg/L to 70.82 μg/L as the time extended from 0 s to 240 s (Fig. 1 (c)).

3.2. Molecular forces

Insights into the interactions holding the MP gels were obtained by mixing the gels with different solvents and measuring the amount of soluble protein (Cao et al., 2018). Around 53.2% of the ionic bonds lost after incubation with PAW_{240} compare to that of the control, the protein solubility declined from 0.23 mg/mL to 0.11 mg/mL ($P < 0.05$). Upon disruption of the hydrogen bonds by NaCl, protein solubility increased significantly ($P < 0.05$) from 0.34 mg/mL of PAW_0 to 0.51 mg/mL of PAW_{30}. However, protein solubility gradually decreased to 0.27 mg/mL ($P < 0.05$) with prolonged PAW treatment. These results revealed that the hydrogen bonds of MP gels can be enhanced in PAW_{30} and PAW_{60} but weakened in PAW_{120} and PAW_{240}. Interestingly, this trend was corresponding with that of WHC (Fig. 4(c)). The hydrogen bonds and electrostatic interactions between MPs and water molecules played important roles in the entrapment of free water in the matrix during gelation process (Li et al., 2019). Therefore, the higher the hydrogen bond content, the better the water retention of the MP gels. It was shown in Fig. 2 that hydrophobic interaction played a dominant role in the formation of MP gel, which was consistent with previous studies (Cao et al., 2018). Simultaneously, incubation with PAW significantly increased the hydrophobic interactions of MP gels, upon disruption of the hydrophobic interactions by urea, protein solubility improved from 0.70 mg/mL to 1.13 mg/mL at PAW_{240} (Fig. 2).

3.3. Protein conformation

Raman scattering spectroscopy is one of the methods that afford information on peptide backbone conformations in protein molecules (Xu et al., 2011). Bands between 1600 cm^{-1} to 1700 cm^{-1} were used to analyze the secondary structures (α-helix, β-sheet, β-turn and random coil) of MPs. With increasing treatment time of PAW, the content of α-helix in MPs gradually decreased from 31.61% to 26.95% ($P < 0.05$). At the same time, the β-sheet significantly ($P < 0.05$) increased from 29.73% to 31.70% (Fig. 3 (a)). These results revealed that PAW modified secondary structures of MPs by inducing the transformation from α-helix and random coil to β-sheet and β-turn, which related to the reactive oxygen (ROS) generated by the Fenton system (Jiang et al., 2020).

Tryptophan (Trp) is an aromatic amino acid, the intrinsic fluorescence measurements characterize changes in Trp residues by scanning the maximum fluorescence intensity (FImax). It was noted that the highest fluorescence intensity was PAW_0, however, the FImax in PAW_{30}, PAW_{60}, PAW_{120} and PAW_{240} decreased by 11.18%, 31.90%, 65.01% and 73.50%, respectively (Fig. 3 (b)). The decrease in IFI was associated with denaturation and exposure of the tryptophan indole side chain, suggesting that prolonged PAW treatment resulted in exposure of buried tryptophan residues and changes in the tertiary structure of MPs (Tan et al., 2022).

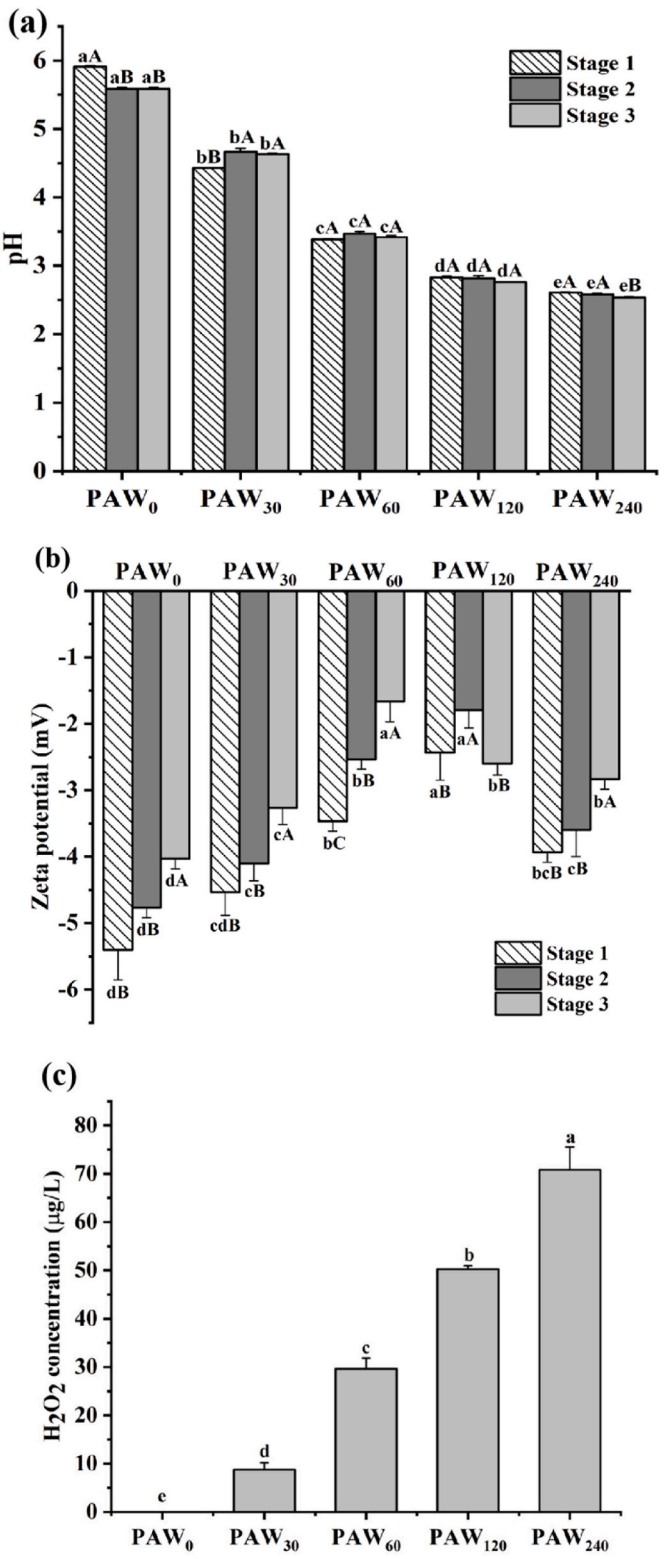

Fig. 1. Effects of PAW on the pH (a), Zeta potential (b) of MP solutions at different heating stages and H_2O_2 concentration of PAW (c). Stage 1, MP solutions without heating; Stage 2, MP solutions heating at 40 °C for 1 h; Stage 3, MP solutions heating at 40 °C for 1 h and 90 °C for 30 min. Graph bars with different letter represent significant difference ($P < 0.05$), where lowercase letters indicate significance of different samples at the same heating treatment, and capital letters indicate significance of the same sample at different heating treatments.

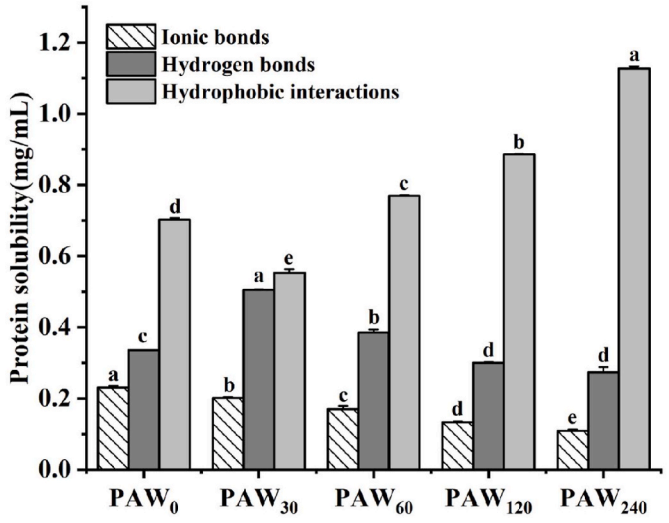

Fig. 2. Effects of PAW on the protein solubilities contributed by ionic bonds, hydrogen bonds and hydrophobic interactions in MP gels. Graph bars with different letter (a-d) represent significant difference ($P < 0.05$).

3.4. Protein aggregation, gel strength and WHC

The change in the absorbance of MPs solution at 340 nm can reflect the different degree of protein aggregation. In the present study, the A_{340} of the control (PAW_0) increased significantly ($P < 0.05$) from 0.06 to 0.31 and 0.33 after Stage 2 and Stage 3 respectively (Fig. 4 (a)). Compared to the A_{340} of PAW_0 at Stage 1 (0.06), that of the PAW_{30}, PAW_{60}, and PAW_{120} significantly ($P < 0.05$) increased to 0.12, 0.18 and 0.12, respectively, suggesting that PAW treated for 30–120 s promoted the aggregation of MPs at Stage 1. Compared to the A_{340} of PAW_0 after Stage 2 or Stage 3, that of the PAW_{60} reached the summit ($P < 0.05$). In addition, the A_{340} of PAW_{30} and PAW_{60} increased significantly ($P < 0.05$) from Stage 1 to Stage 2, but subsequently decreased ($P < 0.05$) after Stage 3. Furthermore, the A_{340} of PAW_{240} was the lowest due to excessive aggregation of MPs (Fig. 4 (a)). A_{340} gradually decreased after PAW_{60} treatment group, which was due to the increase of absorbance value caused by excessive aggregation and sedimentation of protein.

The gel strength of MP gels significantly ($P < 0.05$) increased incubation with PAW from 0 s to 120 s. Compared to the gel strength of PAW_0 (15.16 g mm), the gel strength significantly ($P < 0.05$) increased to 56.05 g mm, and then greatly decreased to 34.75 g mm after PAW_{240} treatment (Fig. 4 (b)). These results indicated that MPs modified with structural changes have optimal time for PAW processing, although PAW significantly ($P < 0.05$) enhanced the gel strength of MP gels, which was consistent with the findings of Nyaisaba et al. (2019).

The WHC increased and then decreased with the treatment time of PAW. In detail, PAW_{30} and PAW_{60} enhanced the WHC of the control from 54.31% to 66.03% and 59.24%, respectively ($P < 0.05$). However, the WHC then declined to 47.44% ($P < 0.05$) when the processing time of PAW was extended until 240 s (Fig. 4 (c)). For the PAW-treated MP gels, the WHC decreased gradually with the increasing treatment time of PAW ($P < 0.05$).

3.5. Dynamic rheology

As shown in Fig. 5 and the Supplementary Table 1, a drastic increase in G′ of the control was observed at 35.8 °C (the first critical turning point, FCTP), which was considered as the onset point or the initial transformation from sol to gel (Xiong et al., 2021). The G′ of control group then increases and reaches a first peak at 40.1 °C (127 Pa) followed by a steep drop to 48.8 °C. Subsequently, G′ increased again from 48.8 °C (the second critical turning point, SCTP) and reached the second

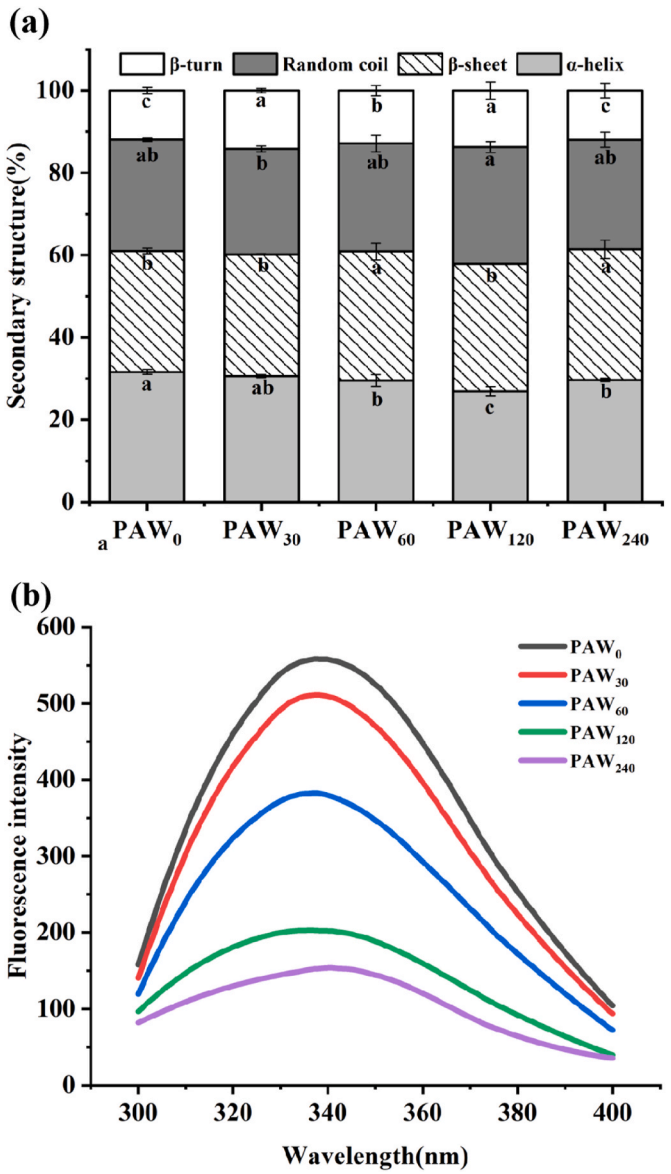

Fig. 3. Effects of PAW on the secondary structure content (a) and intrinsic fluorescence intensity (b) of MPs. Graph bars with different letter (a-d) represent significant difference ($P < 0.05$).

summit (8 Pa) at 90 °C. This finding was consistent with a previous study, in which the second increase in G' symbolized the formation of an irreversible gel network as a result of stronger tail-tail cross-linking between denatured myosin molecules (Singh and Sambyal, 2022). The temperature of the FCTP of PAW_{30}, PAW_{60}, PAW_{120}, and PAW_{240} declined from 35.8 °C in control to 35.2 °C, 34.9 °C, 34.7 °C, and 33.8 °C, respectively (Supplementary Table 1). to observe that the temperature of the SCTP in the PAW-treated group were also decreased than that of the control. Similarly, the temperature of the second peak were also advanced remarkably by PAW.

3.6. CLSM

To further observe the effect of PAW modification on the aggregation degree of MPs, the microstructure of MP gel and its sol was observed by confocal laser scanning microscopy (CLSM) (Tan et al., 2022). The red ones are MPs particles, with the prolongation of PAW treatment, MPs aggregates increased, and the aggregate diameter gradually increased in MP sols. For MP gels, network structures formed. The MPs gels

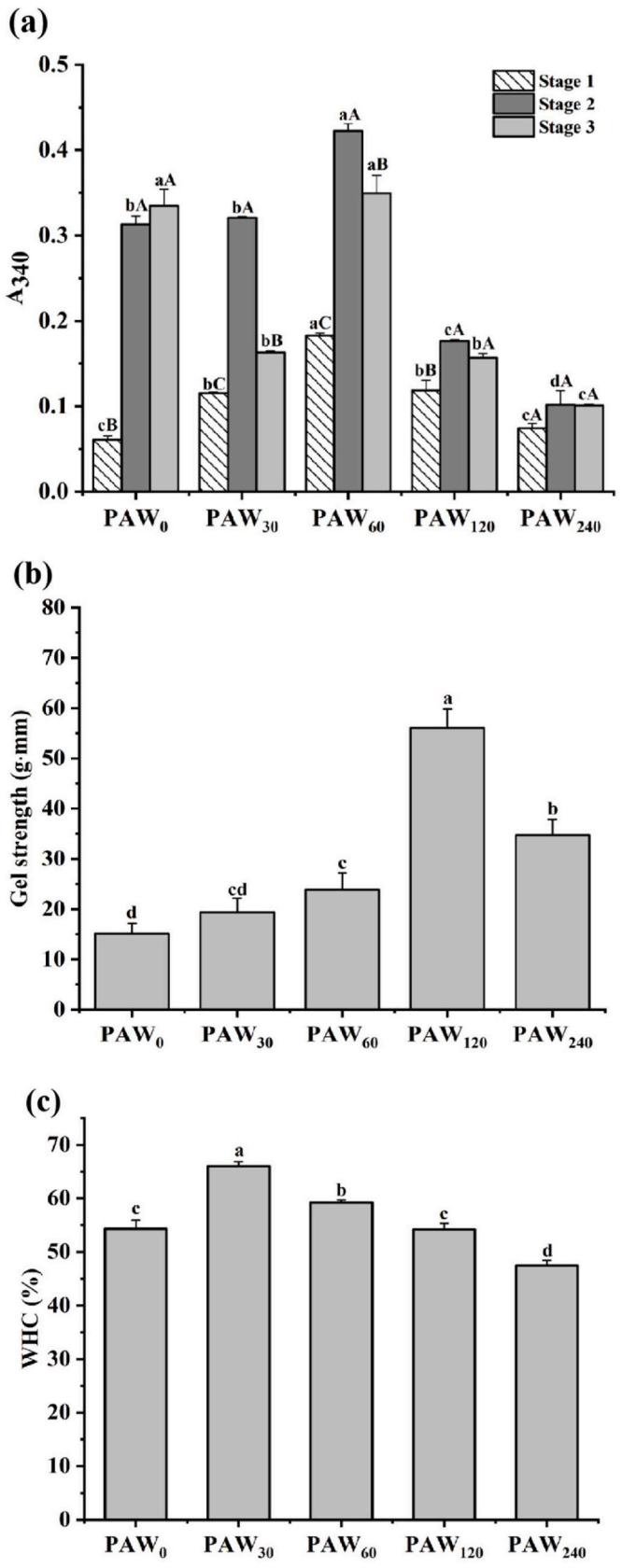

Fig. 4. Effect of PAW on the protein aggregation (a), gel strength (b) and WHC (c) of MP gels. Graph bars with different letter (a-d) represent significant difference ($P < 0.05$).

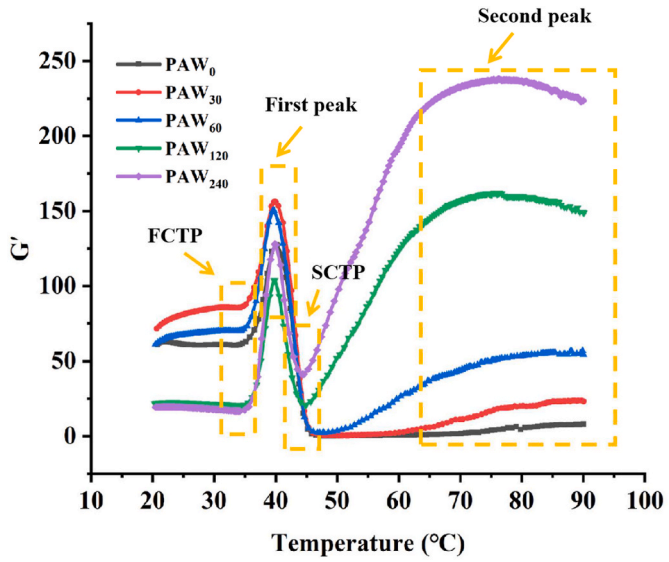

Fig. 5. Effects of PAW on the storage modulus (G′) of MPs during heating. FCTP: the first critical turning point; SCTP: the second critical turning point.

cross-linked more densely as the PAW treatment time increased from 0 s to 60 s. Interestingly, filamentous aggregates due to excessive aggregation of MP gels could be observed in PAW_{120} and PAW_{240} groups (Fig. 6).

4. Discussion

In the present study, the modification of *Aristichthys nobilis* MPs by PAW was investigated and the results showed that as the processing time of PAW increased, the pH and ζ-potential decreased (Fig. 1), the hydrophobic interactions in MP gels increased (Fig. 2), α-helix gradually transformed to β-sheet (Fig. 3 (a)), protein aggregation increased (Figs. 4 and 6). After PAW processing, the increase in hydrophobic interactions and surface hydrophobicity, the enhancement of β-sheet contents (Fig. 3 (a)) and exposure of tryptophan residues (Fig. 3 (b)) indicated formation of protein cross-links and aggregates which improved the gel strength (Fig. 4 (b)) and WHC (Fig. 4 (c)) of MP gels. Based on these results, it was here proposed the modification mechanism of PAW on the secondary structure of MPs and the main intermolecular forces during heating (Fig. 7).

PAW significantly reduced the pH values of the MP solution (Fig. 1 (a)) and MP gel (S. Fig. 2) owing to its acidic property (S. Fig. 1), which was consistent with the previous reports (Qian et al., 2019). Furthermore, the reduction in pH values of MP solutions might be related not only to a certain amount of H_2O_2 (Fig. 1 (c)), NO_2^- and O_3 in the PAW after discharge treatment (Chaijan et al., 2021) but also to proton generation after PAW treatment (Qian et al., 2021). In addition, the minor changes in pH values of PAW_0 after Stage 2 and Stage 3 might be attributed to the structural changes of protein induced by heating (Tan et al., 2022). For the PAW-treated groups, the pH of MP solutions was jointly decided by heating and PAW. However, the ζ-potential of MPs did not change completely with pH, demonstrating that it was not only pH that changed the electrostatic interactions among MP molecules (Fig. 1 (b)). The decreased absolute value of the MPs potential treated with PAW from Stage 1 to Stage 3 indicated that less internal charged groups were exposed on the surface of proteins (Fig. 1 (b)), which weakened the electrostatic repulsion among protein particles (Zhao et al., 2022). Qian et al. (2021) also reported that the decreased negative charge of MPs could decrease the intermolecular repulsion force, promote the protein aggregation (Figs. 4 (a), Fig. 6). Based on this, it was speculated reasonably that besides pH effects induced by PAW, active substances formed during the preparation of PAW might also change the

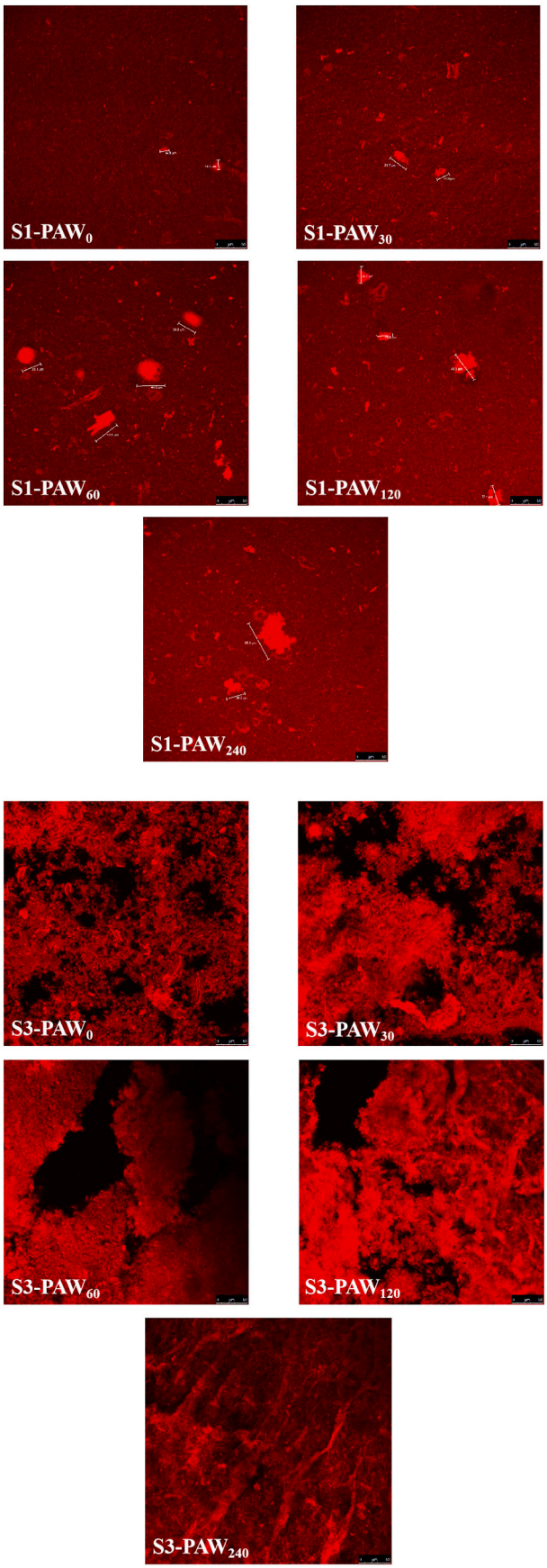

Fig. 6. Effects of PAW on the confocal laser scanning microscopy of MP gel and its sol.

charging of MPs (Ekezie et al., 2019).

In the present study, PAW modified secondary structures of MPs by inducing the transformation from α-helix and random coil to β-sheet and β-turn (Fig. 3 (a)). Furthermore, it was recognized that the treatment of H_2O_2 concentration at 20 mM decreased the α-helix content with the formation of more β-sheet structures (Zhang et al., 2022), which suggested that the change of α-helix and β-sheet content may be due to the small amount of H_2O_2 (Fig. 1 (c)) in PAW. In addition, pH changes in MPs induced by PAW (Fig. 1(a)) were also one of the reasons for the transformation of secondary structure, because it was reported that a large number of hydrophobic groups presented in the α-helix of the myosin tail would be exposed due to the drastic pH fluctuations (Tan et al., 2022). The tertiary network structure of the MP gel was formed by aggregation and cross-linking of exposed hydrophobic amino acid residues during heating (Li et al., 2019). The FI_{max} gradually decreased with increasing the treatment time of PAW (Fig. 3 (b)), indicating that the PAW treatment resulted in the protein unfolding and the exposure of Trp residues buried in the core of protein to the solvent (hydrophilic environment) (Nyaisaba et al., 2019). Generally, the quenching of tryptophan fluorescence was mainly attributed to protein modification and protein-protein cross-linking derived from oxidation (Zhang et al., 2022). In the present study, PAW contained a small amount of H_2O_2 (Fig. 1 (c)) so some degree of protein oxidation, which caused the exposure of hydrophobic groups (Fig. 2) and the formation of protein aggregation (Fig. 4 (a)). In addition, pH was considered as a significant factor in the exposure of hydrophobic amino acid residue (Ni et al., 2014). The gradually decreased pH of PAW solutions with the treatment time (S. Fig. 2) led to the decreased pH of the MP gel (S. Fig. 3).

Protein oxidation and pH changes ultimately led to intramolecular and intermolecular cross-linking and protein aggregation (Fig. 6) (Tan et al., 2022). The G′ of the second peak was enhanced remarkably by PAW from 8 Pa to 237 Pa with its treatment time (Fig. 5, Supplementary Table 1), indicating the improved gelling ability of MPs. This result was validated during the programmed cooling process, where G′ continued to increase with decreasing temperature, indicating a better 3D gel network (Xiong et al., 2021). The change in G′ of MPs during heating implied the unfolding of protein structure and indirectly reflected the process of protein denaturation, aggregation, and spatial network formation (Chen et al., 2018). Based on the results mentioned above, it could be concluded that PAW advanced in the denaturation temperature of MP, then shortened the degradation time of gel, finally enhancing the gel-forming ability of MP (Fig. 4 (b)). In addition, it was believed that ionic bonds were negatively correlated with gel-forming ability (Cao et al., 2018; Shi et al., 2022). Consequently, the weakened ionic bonds induced by PAW contributed to the formation of an ideal gel with enhanced G' (Fig. 5) and gel strength (Fig. 4(b)). Qian et al. (2021) also identified that PAW improved the WHC (Fig. 4 (a)) of CMP gels, which was attributed to the unfolding of MP promoted by PAW and more reactions between water and proteins. The decreased WHC of MP gels treated by PAW from 30 s to 120 s might be due to the increase in gel strength (Fig. 4(b)), since the water inside of gels can be squeezed and lost when the gel strength of MP gels improved (Wang et al., 2021). In general, PAW could effectively improve the gel strength and WHC of MP gels but the treatment time of PAW needed to be reasonably controlled.

5. Conclusion

In the present study, MPs from *Aristichthys nobilis* was extracted using 0.6M NaCl-PAW solution, and the effects of PAW on the protein modifications as well as PAW-modified MPs on the quality of MP gel were studied. In general, PAW declined the pH values of MP solutions and MP gels, which promoted the unfolding of MPs and exposure of Trp residues. Simultaneously, H_2O_2 in PAW also promoted the aggregation of MPs. Subsequently, larger protein aggregates formed gel with higher gel strength and dense microstructure driven by intermolecular forces, especially hydrophobic interactions. Furthermore, dynamic rheology

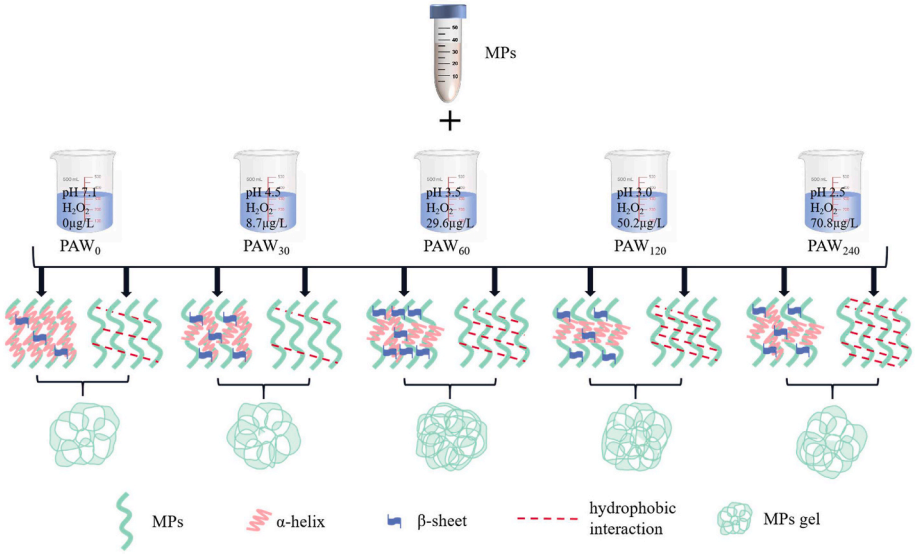

Fig. 7. Proposed mechanism of secondary structure and hydrophobic interaction changes in PAW-modified MPs during heating.

indicated a gradually increased storage modulus and shortened degradation time of MPs with the increasing treatment time of PAW. In conclusion, PAW can be used to improve the quality of freshwater surimi products, and the suggested treatment time was 60–120 s. Despite the present study providing an underlying mechanism of PAW promoting the aggregation and gelation of MPs, much needs to be learned about the more comprehensive mechanism from the point of view of oxidation since some active substances including NO, NO_2, OH•, NO•, and RONS exist in the PAW.

CRediT authorship contribution statement

Mengzhe Li: Formal analysis, Methodology, Writing – original draft, Software. **Tong Shi:** Writing – review & editing, Supervision, Data curation. **Xin Wang:** Methodology, Investigation, Data curation. **Yulong Bao:** Writing – review & editing. **Zhiyu Xiong:** Validation, Data curation. **Abdul Razak Monto:** Writing – review & editing. **Wengang Jin:** Project administration. **Li Yuan:** Funding acquisition, Project administration, Conceptualization. **Ruichang Gao:** Writing – review & editing, Project administration, Conceptualization.

Declaration of competing interest

The authors declare that they have no known competing financial interests or personal relationships that could have appeared to influence the work reported in this paper.

Acknowledgments

This work was supported by the National Natural Science Foundation of China (U20A2067). This work was supported by the 2021 Jiangsu Postgraduate Practice Innovation Program (SJCX21_1720).

Appendix A. Supplementary data

Supplementary data to this article can be found online at https://doi.org/10.1016/j.crfs.2022.09.003.

References

Cao, H.W., Fan, D.M., Jiao, X.D., Huang, J.L., Zhao, J.X., Yan, B.W., Zhou, W.G., Zhang, W.H., Zhang, H., 2018. Effects of microwave combined with conduction heating on surimi quality and morphology. J. Food Eng. 228, 1–11. https://doi.org/10.1016/j.jfoodeng.2018.01.021.

Chaijan, M., Chaijan, S., Panya, A., Nisoa, M., Cheong, L.-Z., Panpipat, W., 2021. High hydrogen peroxide concentration-low exposure time of plasma-activated water (PAW): a novel approach for shelf-life extension of Asian sea bass (Lates calcarifer) steak. Innov Food Sci Emerg 74. https://doi.org/10.1016/j.ifset.2021.102861.

Chen, X., Xu, X., Liu, D.M., Zhou, G.H., Han, M.Y., Wang, P., 2018. Rheological behavior, conformational changes and interactions of water-soluble myofibrillar protein during heating. Food Hydrocolloids 77, 524–533. https://doi.org/10.1016/j.foodhyd.2017.10.030.

Ekezie, F.C., Cheng, J.H., Sun, D.W., 2019. Effects of atmospheric pressure plasma jet on the conformation and physicochemical properties of myofibrillar proteins from king prawn (Litopenaeus vannamei). Food Chem. 276, 147–156. https://doi.org/10.1016/j.foodchem.2018.09.113.

Fang, Q., Shi, L., Ren, Z.Y., Hao, G.X., Chen, J., Weng, W.Y., 2021. Effects of emulsified lard and TGase on gel properties of threadfin bream (Nemipterus virgatus) surimi. LWT (Lebensm.-Wiss. & Technol.) 146. https://doi.org/10.1016/j.lwt.2021.111513.

Gao, R.C., Shi, T., Sun, Q.C., Li, X., McClements, D.J., Yuan, L., 2019. Effects of l-arginine and l-histidine on heat-induced aggregation of fish myosin: bighead carp (Aristichthys nobilis). Food Chem. 295, 320–326. https://doi.org/10.1016/j.foodchem.2019.05.095.

Jiang, S., Zhao, S.C., Jia, X.W., Wang, H., Zhang, H., Liu, Q., Kong, B.H., 2020. Thermal gelling properties and structural properties of myofibrillar protein including thermo-reversible and thermo-irreversible curdlan gels. Food Chem. 311, 126018 https://doi.org/10.1016/j.foodchem.2019.126018.

Jiao, X.D., Cao, H.W., Fan, D.M., Huang, J.L., Zhao, J.X., Yan, B.W., Zhou, W.G., Zhang, W.H., Zhang, H., 2019. Effects of fish oil incorporation on the gelling properties of silver carp surimi gel subjected to microwave heating combined with conduction heating treatment. Food Hydrocolloids 94, 164–173. https://doi.org/10.1016/j.foodhyd.2019.03.017.

Karimi, F., Hamidian, Y., Behrouzifar, F., Mostafazadeh, R., Ghorbani-HasanSaraei, A., Alizadeh, M., Naderi Asrami, P., 2022. An applicable method for extraction of whole seeds protein and its determination through Bradford's method. Food Chem. Toxicol. 164, 113053 https://doi.org/10.1016/j.fct.2022.113053.

Klassen, N.V., Marchlngton, David, McGowan, H.C.E., 1994. H202 determination by the I3 method and by KMn04 titration. Anal. Chem. 66, 2921–2925.

Kong, W.J., Zhang, T., Feng, D.D., Xue, Y., Wang, Y.M., Li, Z.J., Yang, W.G., Xue, C., 2016. Effects of modified starches on the gel properties of Alaska Pollock surimi subjected to different temperature treatments. Food Hydrocolloids 56, 20–28. https://doi.org/10.1016/j.foodhyd.2015.11.023.

Laurita, R., Gozzi, G., Tappi, S., Capelli, F., Bisag, A., Laghi, G., Gherardi, M., Cellini, B., Abouelenein, D., Vittori, S., Colombo, V., Rocculi, P., Dalla Rosa, M., Vannini, L., 2021. Effect of plasma activated water (PAW) on rocket leaves decontamination and nutritional value. Innov Food Sci Emerg 73. https://doi.org/10.1016/j.ifset.2021.102805.

Li, F.F., Wang, B., Kong, B.H., Shi, S., Xia, X.F., 2019a. Decreased gelling properties of protein in mirror carp (Cyprinus carpio) are due to protein aggregation and structure deterioration when subjected to freeze-thaw cycles. Food Hydrocolloids 97. https://doi.org/10.1016/j.foodhyd.2019.105223.

Li, Z.Y., Wang, J.Y., Zheng, B.D., Guo, Z.B., 2019b. Effects of high pressure processing on gelation properties and molecular forces of myosin containing deacetylated konjac glucomannan. Food Chem. 291, 117–125. https://doi.org/10.1016/j.foodchem.2019.03.146.

Liao, X.Y., Su, Y., Liu, D.H., Chen, S.G., Hu, Y.Q., Ye, X.Q., Wang, J., Ding, T., 2018. Application of atmospheric cold plasma-activated water (PAW) ice for preservation

of shrimps (Metapenaeus ensis). Food Control 94, 307–314. https://doi.org/10.1016/j.foodcont.2018.07.026.

Ma, Y.L., Xiong, S.B., You, J., Hu, Y., Huang, Q.L., Yin, T., 2018. Effects of vacuum chopping on physicochemical and gelation properties of myofibrillar proteins from silver carp (Hypophthalmichthys molitrix). Food Chem. 245, 557–563. https://doi.org/10.1016/j.foodchem.2017.10.139.

Maqsood, S., Benjakul, S., Shahidi, F., 2013. Emerging role of phenolic compounds as natural food additives in fish and fish products. Crit. Rev. Food Sci. Nutr. 53 (2), 162–179. https://doi.org/10.1080/10408398.2010.518775.

Ni, N., Wang, Z.Y., He, F., Wang, L.C., Pan, H., Li, X., Wang, Q., Zhang, D.Q., 2014. Gel properties and molecular forces of lamb myofibrillar protein during heat induction at different pH values. Process Biochem. 49 (4), 631–636. https://doi.org/10.1016/j.procbio.2014.01.017.

Nikolantonaki, M., Magiatis, P., Waterhouse, A.L., 2014. Measuring protection of aromatic wine thiols from oxidation by competitive reactions vs wine preservatives with ortho-quinones. Food Chem. 163, 61–67. https://doi.org/10.1016/j.foodchem.2014.04.079.

Nyaisaba, B.M., Miao, W., Hatab, S., Siloam, A., Chen, M., Deng, S., 2019. Effects of cold atmospheric plasma on squid proteases and gel properties of protein concentrate from squid (Argentinus ilex) mantle. Food Chem. 291, 68–76. https://doi.org/10.1016/j.foodchem.2019.04.012.

Qian, J., Zhuang, H., Nasiru, M.M., Muhammad, U., Zhang, J.H., Yan, W.J., 2019. Action of plasma-activated lactic acid on the inactivation of inoculated Salmonella Enteritidis and quality of beef. Innov Food Sci Emerg 57. https://doi.org/10.1016/j.ifset.2019.102196.

Qian, J., Wang, Y.Y., Zhuang, H., Yan, W.J., Zhang, J.H., Luo, J., 2021a. Plasma activated water-induced formation of compact chicken myofibrillar protein gel structures with intrinsically antibacterial activity. Food Chem. 351, 129278 https://doi.org/10.1016/j.foodchem.2021.129278.

Qian, S., Dou, P.P., Wang, J.L., Chen, L., Xu, X.L., Zhou, G.H., Zhu, B.W., Niamat, U., Feng, X.C., 2021b. Effect of MTGase on silver carp myofibrillar protein gelation behavior after peroxidation induced by peroxyl radicals. Food Chem. 349, 129066 https://doi.org/10.1016/j.foodchem.2021.129066.

Qiu, C.J., Xia, W.S., Jiang, Q.X., 2013. Effect of high hydrostatic pressure (HHP) on myofibril-bound serine proteinases and myofibrillar protein in silver carp (Hypophthalmichthys molitrix). Food Res. Int. 52 (1), 199–205. https://doi.org/10.1016/j.foodres.2013.03.014.

Shi, J., Lei, Y.T., Shen, H.X., Hong, H., Yu, X.P., Zhu, B.W., Luo, Y.K., 2019. Effect of glazing and rosemary (Rosmarinus officinalis) extract on preservation of mud shrimp (Solenocera melantho) during frozen storage. Food Chem. 272, 604–612. https://doi.org/10.1016/j.foodchem.2018.08.056.

Shi, T., Xiong, Z.Y., Jin, W.G., Yuan, L., Sun, Q.C., Zhang, Y.H., Li, X.T., Gao, R.C., 2020. Suppression mechanism of l-arginine in the heat-induced aggregation of bighead carp (Aristichthys nobilis) myosin: the significance of ionic linkage effects and hydrogen bond effects. Food Hydrocolloids 102. https://doi.org/10.1016/j.foodhyd.2019.105596.

Shi, T., Wang, X., Li, M.Z., Xiong, Z.Y., McClements, D.J., Bao, Y.L., Song, T., Li, J., Yuan, L., Jin, W.G., Gao, R.C., 2022. Mechanism of low-salt surimi gelation induced by microwave heating combined with l-arginine and transglutaminase: on the basis of molecular docking between l-arginine and myosin heavy chain. Food Chem. 391, 133184 https://doi.org/10.1016/j.foodchem.2022.133184.

Singh, R.V., Sambyal, K., 2022. An overview of β-carotene production: current status and future prospects. Food Biosci. 47 https://doi.org/10.1016/j.fbio.2022.101717.

Song, T., Xiong, Z.Y., Shi, T., Yuan, L., Gao, R.C., 2022. Effect of glutamic acid on the preparation and characterization of Pickering emulsions stabilized by zein. Food Chem. 366, 130598 https://doi.org/10.1016/j.foodchem.2021.130598.

Tan, M.T., Ding, Z.Y., Mei, J., Xie, J., 2022. Effect of cellobiose on the myofibrillar protein denaturation induced by pH changes during freeze-thaw cycles. Food Chem. 373 (Pt B), 131511 https://doi.org/10.1016/j.foodchem.2021.131511.

Wang, J.Y., Li, Z.Y., Zheng, B.D., Zhang, Y., Guo, Z.B., 2019. Effect of ultra-high pressure on the structure and gelling properties of low salt golden threadfin bream (Nemipterus virgatus) myosin. LWT (Lebensm.-Wiss. & Technol.) 100, 381–390. https://doi.org/10.1016/j.lwt.2018.10.053.

Wang, X., Wang, L.M., Yang, K., Wu, D., Ma, J., Wang, S.J., Zhang, Y.H., Sun, W.Q., 2021. Radio frequency heating improves water retention of pork myofibrillar protein gel: an analysis from water distribution and structure. Food Chem. 350, 129265 https://doi.org/10.1016/j.foodchem.2021.129265.

Xiong, G.Q., Cheng, W., Ye, L.X., Du, X., Zhou, M., Lin, R.T., Geng, S.R., Chen, M.L., Corke, H., Cai, Y.-Z., 2009. Effects of konjac glucomannan on physicochemical properties of myofibrillar protein and surimi gels from grass carp (Ctenopharyngodon idella). Food Chem. 116 (2), 413–418. https://doi.org/10.1016/j.foodchem.2009.02.056.

Xiong, Z.Y., Shi, T., Zhang, W., Kong, Y.F., Yuan, L., Gao, R.C., 2021. Improvement of gel properties of low salt surimi using low-dose l-arginine combined with oxidized caffeic acid. LWT (Lebensm.-Wiss. & Technol.) 145. https://doi.org/10.1016/j.lwt.2021.111303.

Xu, X.L., Han, M.Y., Fei, Y., Zhou, G.H., 2011. Raman spectroscopic study of heat-induced gelation of pork myofibrillar proteins and its relationship with textural characteristic. Meat Sci. 87 (3), 159–164. https://doi.org/10.1016/j.meatsci.2010.10.001.

Zhang, M., Li, C., Zhang, Y., Pan, J., Huang, S., He, L.C., Jin, G., 2022. Impact of salt content and hydrogen peroxide-induced oxidative stress on protein oxidation, conformational/morphological changes, and micro-rheological properties of porcine myofibrillar proteins. Food Chem. 370, 131074 https://doi.org/10.1016/j.foodchem.2021.131074.

Zhao, X.C., Qi, J., Fan, C.X., Wang, B., Yang, C., Liu, D.Y., 2022. Ultrasound treatment enhanced the ability of the porcine myofibrillar protein to bind furan compounds: Investigation of underlying mechanisms. Food Chem. 384, 132472 https://doi.org/10.1016/j.foodchem.2022.132472.